

Materials balance in primary batteries.

V. Scaling up of lithium inorganic batteries

N. MARINČIĆ, F. GOEBEL

GTE Laboratories, Inc. Waltham, Massachusetts, USA

Received 14 March 1977

Modified design procedures are described for large rectangular cells, since the procedures developed for small cylindrical cells [1-4] were found inapplicable in the optimization of scaled-up units. Discharge data are presented for cells several orders of magnitude larger than the standard *D* cell, showing a good agreement between the predicted and realized cell capacity. A remarkable increase in the energy density has been achieved with increase in the cell size, well in excess of 600 Wh kg^{-1} at low discharge rates. The definition of some intrinsic characteristics of the system [such as the value of k_3 , ($\text{cm}^3 \text{ A h}^{-1}$)] has been confirmed with a greater accuracy using the data obtained with these large cells.

1. Introduction

The study of the materials balance in small cylindrical cells has been completed for the cells made with the Li/SOCl_2 primary system for both the low rate type cells with the simplest construction [1] and the high rate type cells with a more elaborate wound electrode construction [2]. The performance of these cells on discharge was found to be in very good agreement with the characteristics predicted by the cell design. A computer-aided design procedure, developed for the wound cell construction [3], proved to be an efficient means for the accurate prediction of the cell behaviour in a wide range of discharge rates. The applicability of the procedures to a wide variety of lithium batteries with organic electrolytes has also been demonstrated [4].

Two basic assumptions were made in this study. The first one was that the electrolyte is present in the cell in sufficient quantity at all times during the discharge of the cell. The assumption proved valid for all systems using organic solvents [4], or liquid depolarizers alone (Li/SOCl_2), since the electrolyte either does not participate in the discharge reaction at all (organics) or is present in a large excess over the stoichiometric quantity required for other reasons (porosity). The assumption proved false in systems using a mixture of organic solvents and liquid

depolarizers (Li/SO_2 system) since, in an optimized electrode structure, starved electrolyte conditions are reached before the discharge capacity of the electrode structure was exhausted.

The second assumption was that the electrolyte would be uniformly distributed throughout the electrode structure, maintaining flooded conditions at all times during discharge in spite of the inevitable volume reduction of active components during discharge, and irrespective of the orientation of the cell. This condition was easily fulfilled with small cells, due to the capability of porous electrodes to attract and hold the electrolyte above the level outside the electrodes in the cells not exceeding the commercial *D* size. This assumption no longer held when the cell size was increased in the first scale-up step described below. These and some other limitations of this design in the scaled-up version of cylindrical cells are discussed below, before the modified optimization procedure is presented.

The simplest design for cylindrical cells has been worked out [1] for the low discharge rate, whereby a concentric configuration of electrodes has been selected. An electrode structure of overall diameter (D) and height (H) was considered, leading to the simple set of expressions defining the internal diameter of the lithium anode (D_1) and the internal diameter of the cathode (D_2) in terms of the overall diameter of the electrode

package D for the maximum cell capacity Q :

$$D_1 = 0.875D \quad (1)$$

$$D_2 = 0.466D \quad (2)$$

$$Q = 0.304D^2H. \quad (3)$$

The above expressions represent a special case already including the stoichiometric characteristics of the cell discharge reactions, as well as the experimentally established value characterizing a particular type of carbon electrodes used. The *post mortem* analysis of a large cylindrical cell showed that the upper section of the cathode reaches the electrolyte starvation half-way through discharge, as the electrolyte level drops, due to the volume reduction of active components. The only way we could extract the predicted capacity from these cells was periodically to change the position of the cell from right-side up to the upside-down position. This was an indication that future designs of large cells would have to provide for a total flooding of the electrodes without depending on the porous electrode structure to attract and hold the electrolyte.

The dimensions and other design parameters of the cylindrical cell used in the first scale-up step were as follows: overall cell size = 7.104 dia. \times 11.179 high (cm); electrode structure = 6.900 dia. \times 10.500 high (cm); cathode O.D. (anode I.D.) = $D_1 = 6.037$ cm; cathode I.D. = $D_2 = 3.215$ cm; cell capacity (predicted) = $Q = 151.97$ A h; cell weight = 832 g; cell volume = 467 cm³.

A typical performance of this cell is shown in the discharge diagram in Fig. 1, while the capacities obtained in various steps of discharge are shown in Table 1. A total capacity of 166.19 A h was obtained, and the energy density was calculated from the portions of the discharge diagram and the

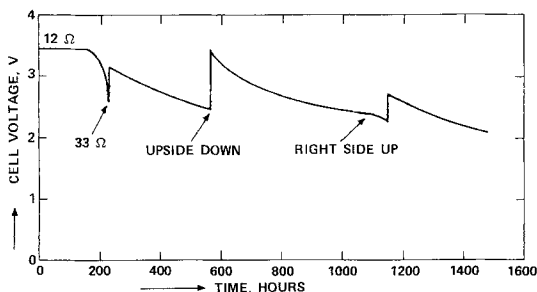


Fig. 1. Discharge curve of the 150 A h cell.

cell weight and volume to be 581 Wh kg⁻¹ or 1030 Wh dm⁻³.

A completed 150 A h cell is shown in Fig. 2. The tests with these cells confirmed that fairly thick carbon electrodes could be efficiently discharged at low rates, even when facing lithium anodes on one side only. A photograph of a spent cathode is shown in Fig. 3, broken in two parts to show the internal structure and the products of discharge precipitated within the voids of the cathode. Conglomerates of sulphur

Table 1. Discharge rates and the capacity obtained for 150 A h cylindrical cell

Load Ω	Average voltage (V)	Average current (mA)	Time (h)	Capacity (A h)	Energy (Wh)
12	3.25	27.9	232	64.73	216.84
33	2.78	84.2	336	28.29	78.65
33	2.70	81.8	576	47.11	127.21
33	2.35	71.2	336	26.06	61.24
Total				166.19	483.94

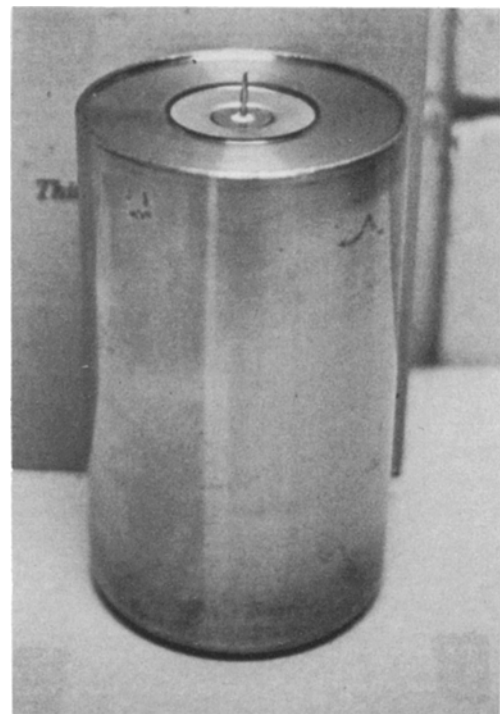


Fig. 2. 150 A h cell.

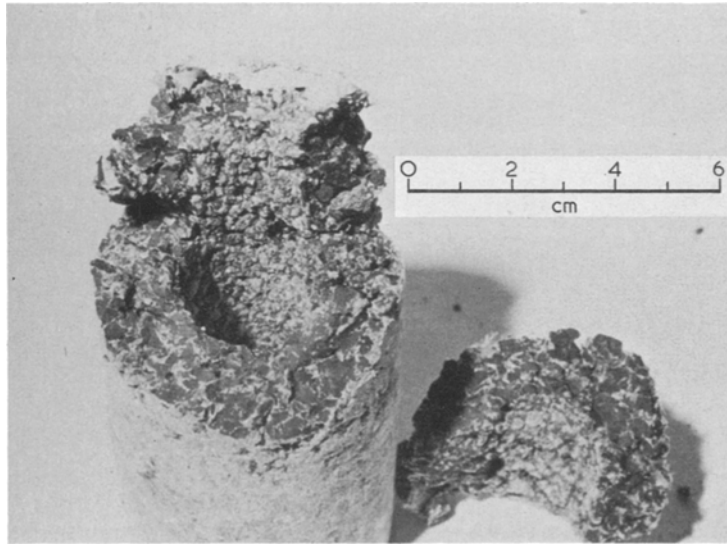


Fig. 3. Structure of a spent cathode (150 Ah cell).

are more easily visible than the precipitates of salts which seem to be much better distributed within the carbon pores.

Another assumption made in the design work for cylindrical cells was that the change in ratio of the active surface areas of cathodes and anodes during discharge would not significantly influence the performance of the cell. The assumption was found to be valid at extremely low discharge rates only. Since the anode and the cathode reaction fronts move apart as the discharge proceeds, the ratio of the surface areas changes in favour of the anode in the concentric cell configuration. This and other difficulties experienced with the large cylindrical cell design indicated that the proper design would be a parallel plate construction, and that the design procedure would have to be modified to ensure the functioning of that electrode structure.

2. Optimization of rectangular cells

A general solution of the problem of space allocation within a rectangular cell must be considered. The volume distribution is schematically presented in Fig. 4. The volume of a single cell (V) must be divided into two portions: one for the electrode structure (V_{st}), and one for the extra electrolyte on top of the electrode structure (V_{ee})

to ensure flooding of the structure throughout discharge, in spite of the volume reduction:

$$V = V_{ee} + V_{st}. \tag{4}$$

The volume of the extra electrolyte can be expressed in terms of the cell capacity Q (Ah) and the specific volume reduction on discharge k_3 [$\text{cm}^3 \text{Ah}^{-1}$]:

$$V_{ee} = k_3 Q. \tag{5}$$

The volume of the electrode structure consists of the volume of the cathode, V_c , the volume of the anodes, V_a , the volumes of the anode and

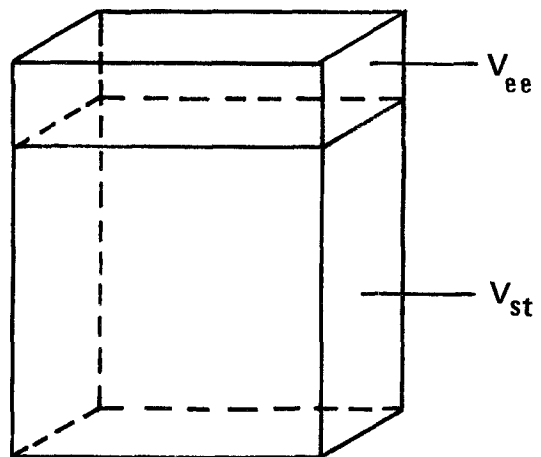


Fig. 4. Volume distribution within a rectangular cell.

cathode current collectors, V_{cs} and V_{as} and the volume of the separators, V_s .

$$V_{st} = V_c + V_a + V_{cs} + V_{as} + V_s. \quad (6)$$

The volume of the cathodes can be expressed in terms of the cell capacity, Q , with the specific capacity of carbon blend, k_2 ($A\ h\ g^{-1}$), the cathodes' porosity P_c , and the density of carbon d_c :

$$V_c = \frac{Q}{k_2 d_c (1 - P_c)}. \quad (7)$$

The volume of the anodes can be expressed in terms of the capacity, Q , with the atomic weight of anode metal, M , the number of electrons per gram-atom involved in the discharge reactions, n , the density of the anode metal, d_a ($g\ cm^{-3}$), the excess factor, E , and the Faraday constant, F ($A\ h\ equiv.^{-1}$):

$$V_a = \frac{MQE}{nF d_a}. \quad (8)$$

The volume of the current collectors and separators can be determined on the basis of the total surface area of electrodes required, which in turn is a function of the maximum discharge current, I (mA), and the maximum allowable current density, i ($mA\ cm^{-2}$). Therefore, for the selected equivalent thickness of cathode current collector t_{cs} , the anode current collectors t_{as} and the separators t_s , the respective volumes are:

$$V_{cs} = \frac{I}{2i} t_{cs} \quad (9)$$

$$V_{as} = \frac{I}{2i} t_{as} \quad (10)$$

$$V_s = \frac{I}{i} t_s. \quad (11)$$

With Equations 6–8, the volume of the electrode structure could be expressed as follows:

$$V_{st} = Q \frac{1}{k_2 d_c (1 - P)} + \frac{ME}{nF d_a} + \frac{I}{2i} (t_{cs} + t_{as} + 2t_s). \quad (12)$$

This equation with Equations 4 and 5 results in:

$$Q = \frac{V - I(t_{cs} + t_{as} + 2t_s)/2i}{k_3 + 1/[k_2 d_c (1 - P)] + ME/nF d_a}. \quad (13)$$

Equation 13 permits the calculation of the cell capacity as a function of the total cell volume, provided that the stoichiometric characteristics of the discharge reaction k_1 (included in P) and k_3 are known, and also provided that the specific cathode capacity k_2 is experimentally determined for the particular cathode material used. The decision must be made regarding the current collectors, separators, and a maximum discharge current density on the basis of previous experience, before one can proceed with the calculation. Once the cell capacity, Q , is determined, the volume of extra electrolyte and the volume of the electrolyte structure can be calculated from Equations 5 and 4 respectively.

The thickness of the cathode plates can be calculated from the total volume of the cathodes, V_c , and their total required surface area, $I/2i$ (counting both sides):

$$t_c = \frac{2iV_c}{I}$$

while the number of individual cathodes (N) is determined from the total surface area required, and the surface area of the electrode that fits the selected shape of the container. The number of plates is a round, whole number on the higher side of the exact value of N calculated. It is necessary to recalculate the electrode thickness based on the total surface area of all plates after their number has been established.

The thickness of anodes is determined next from the total anode volume V_a and the total surface area required to match the surface area of the cathode. The end plates are only one-half as thick as the rest of the plates, but since the number of plates in this case must be $N + 1$, the total volume calculated is not affected by this arrangement.

The total volume of the electrolyte consists of two parts; the extra electrolyte on top of the structure and the portion contained in the pores of the cathode and separators. In most cases the portion contained in the separators can be neglected in relation to that contained in the cathodes. The total can, therefore, be calculated as follows:

$$V_T = k_3 Q + V_c P_c.$$

In some cases, where relatively thin cathodes are used in conjunction with fluffy thick separators, the amount of the electrolyte taken up by the separator must be determined from the porosity of separator and its volume, in the same manner as for the cathodes.

3. Cell design

The present state of the art enables the construction of small cells with predictable characteristics. We have demonstrated in the preceding section that the design theory developed for a certain size cell may not be valid for larger cells, since the numerous assumptions made no longer hold. We have shown that the scale up by a factor of 10 from the standard D size cell to the 150 Ah cell has led to a problem of electrolyte supply at some sections of the cathode. One could assume that this problem will not be present in the stationary cells having the extra electrolyte placed on top of the electrode structure, but one might expect some other similar problems to appear. For this reason one should start the development of the rectangular cells, one step at a time, and thus establishing the basic cell performance parameters for each cell sizes involved.

We have started the scale-up programme with a rectangular cell of the following dimensions: $407 \times 315.5 \times 53.5$ mm (6870 cm³). After allowing for the wall thickness of the container and the tolerance required for a smooth assemblage, the useful cell volume was determined to be 6233 cm³.

In order to avoid the effect of the anode passivation with too low an electrode surface area, and, also the excessive power capability with electrode surface area higher than necessary, it was decided that the current density should not exceed 2 mA cm⁻². It was also decided that such a cell should be discharged at 12 A maximum. With the selection of these and other construction parameters (shown below), one could calculate the maximum cell capacity using Equation 13:

$$Q = \frac{V - I(t_{cs} + t_{as} + 2t_s)/2i}{k_3 + 1/[k_2 d_c(1 - P_c)] + ME/nFd_a}$$

$$= 2179 \text{ Ah.}$$

where: $V = 6233$ cm³; $I = 12000$ mA; $i = 2$ mA cm⁻²; $t_{cs} = 0.05$ cm; $t_{as} = 0.05$ cm; $t_s = 0.10$ cm; $k_2 = 2.00$ Ah g⁻¹; $k_3 = 0.5643$ cm³ (Ah⁻¹); $d_x = 1.95$ g cm⁻³; $d_a = 0.534$ g cm⁻³; $P_c = k_2 d_c / (k_1 \epsilon + k_2 d_c) = 0.799$; $M = 6.935$ g mol⁻¹; $E = 1.25$; $n = 1$; and $F = 26.8$ Ah equiv.⁻¹. With the cell capacity known and with the specific volume reduction on discharge (k_3), one could calculate the volume of the extra electrolyte needed on top of the electrode structure to compensate for the volume reduction; i.e. to ensure the flooding of the electrodes:

$$V_{ee} = k_3 Q = 1229 \text{ cm}^3.$$

The difference between the total cell volume and the volume of the free electrolyte is available for placing the electrode structure. With these volume figures, the dimensions of the cell and the maximum current density set at 2 mA cm⁻² it was possible to calculate that such a cell should have three cathode plates, two full thickness anodes and two half-thickness anodes as end plates. The respective thicknesses of the plates were calculated from the capacity of the cell (Q) taking into account the equivalent thicknesses [2] of the current collectors selected. The total amount of electrolyte was calculated by adding the volume of free electrolyte to the volume required to fill the pores within cathodes and separators. A reasonable effort was made to produce the components having dimensional and other characteristics as close to the predicted figures as possible. Obviously, any deviations from the values established by design would be expected to reduce the cell capacity obtained. The difference between the predicted and the realized capacity could be used to judge the skill and precision with which the components are made and the cells assembled in a fixed volume of the container.

The electrode structure is situated in a stainless steel container, hermetically welded to the cell cover. The cover sub-assembly carries the terminal feedthroughs and the electrolyte filling port. The hermeticity of the components of the cover sub-assembly has been helium tested to pass a 10^{-9} cc atm⁻¹ s⁻¹ requirement.

4. Test results

The cells were discharged under constant load con-

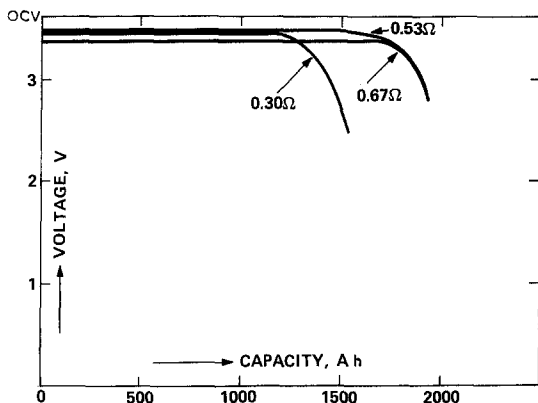


Fig. 5. Discharge characteristics of a 2000 A h cell.

ditions. Three typical discharge curves are shown in Fig. 5, representing the cell voltage as a function of the capacity obtained for three different rates of discharge. The curves for 0.30 and 0.53 Ω were obtained with the cells that incorporated some improvements in the cell internal impedance, relative to the one used in the discharge at 0.67 Ω . Although the differences in operating voltage do not seem large in the diagram, they are significant, when the operating voltage is close to the open circuit voltage. The drop in voltage from the open circuit value of 3.66 V to the operating level provides a good indication of the rate of heat generation in the cell, which is an important engineering consideration in the use of large cells.

The maximum capacity obtained in the tests is within 10% of the predicted value, but only at discharge rates lower than that assumed in the design. The discharge at higher rates, such as the one with a 0.30 Ω load (approximately 11 A) resulted in a significant loss in capacity, probably due to a non-uniform plugging of cathode pores with discharge products at various distances from the anode, as suggested recently [5]. The non-uniformity is expected to be much more pronounced at extreme thicknesses of cathodes and higher current densities.

The design procedure for rectangular cells was used in scaling up the cell size further, leading to the construction of cells with a nominal capacity of 12 000 A h. The discharge curve of such cells at an early stage of development is shown in Fig. 6. Five cells, discharged in series, delivered 10 000 A h at the rate of 28 A. The discharge was terminated when the first cell reached 2 V. The battery was

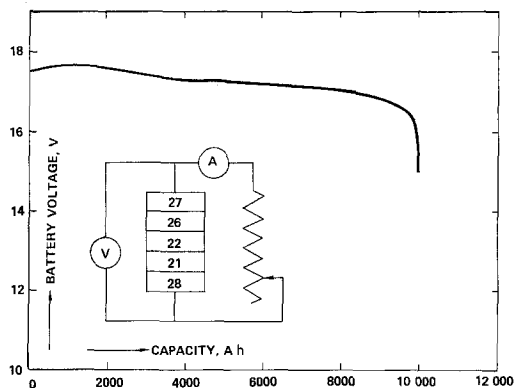


Fig. 6. Discharge curve of a 12 000 A h five cell battery.

dis-assembled and the discharge of the rest of the cells was continued individually in order to establish the statistical spread in the capacities obtained from the cells produced in the same batch, maintaining the same cut-off voltage line. The minimum capacity of 10 000 A h obtained from the weakest of five cells represents a significant result, considering the fact that the cells represented an early state of the scale-up programme. The energy density obtained with these cells is among the highest ever reported for any primary cell: 600 Wh kg^{-1} and 1105 Wh dm^{-3} . A photograph of these large cells is shown in Fig. 7.

The test results reported here are only a part of those generated in the course of the development of the scaled-up primary cells using the lithium/thionyl chloride electrochemical system. The prospects appear rather promising for the use of these cells in many applications. These cells can

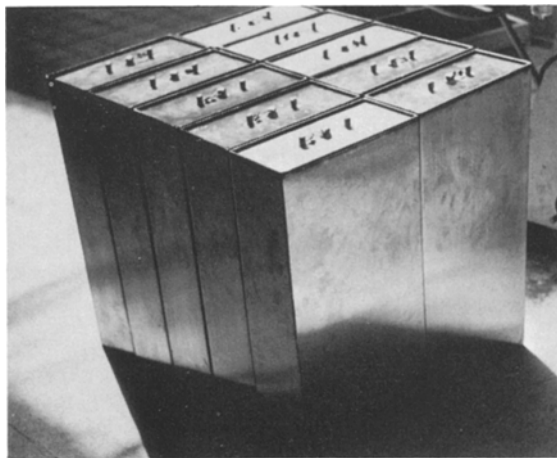


Fig. 7. 12 000 A h cells.

deliver an energy equivalent to 20–25 full charge–discharge cycles of lead-acid batteries of the same volume and with less than 50% of the weight of the lead-acid batteries, with no service costs such as that encountered with the charging and maintenance of lead-acid batteries. There are many applications in which the rechargeability of the lead-acid batteries is not used to the fullest i.e. the total energy delivered in the life of these batteries amounts to less than the equivalent of 20 full cycles. There are other applications in which the maintenance costs of lead acid batteries are so large, because of the distances involved or inaccessibility, that the use of primary maintenance free batteries of large capacity becomes fully justified. In still other applications, a power source cannot be allowed to release any corrosive gases or liquids, because of the damage these agents can do to the instrumentation and circuitry present. Lithium/thionyl chloride batteries, designed to operate at low rates, can be made totally hermetic and will remain so in use or storage, as has been demonstrated in the last three years by the use of

small cells in cardiac pacemakers. The large cells described here, could not have been made in rectangular containers if there was any significant pressure build-up either on storage or in discharge. The scale-up efforts are being continued.

Acknowledgement

The authors are indebted to GTE Sylvania, CSD for the continuous support of this programme and to GTE Laboratories Inc. for permission to publish this paper.

References

- [1] N. Marinčič, *J. Appl. Electrochem.* 5 (1975) 313.
- [2] *Idem, ibid* 6 (1976) 51.
- [3] *Idem, ibid* 6 (1976) 263.
- [4] *Idem, ibid* 6 (1976) 463.
- [5] A. N. Dey and P. Bro, Proc. 10th Int. Power Sources Symp. Brighton, England, September (1976).